

Untethered Feel-Through Haptics Using 18- μm Thick Dielectric Elastomer Actuators

Xiaobin Ji, Xinchang Liu, Vito Cacucciolo, Yoan Civet, Alae El Haitami, Sophie Cantin, Yves Perriard, and Herbert Shea*

Head-mounted displays for virtual reality (VR) and augmented reality (AR) allow users to see highly realistic virtual worlds. The wearable haptics that enable feeling and touching these virtual objects are typically bulky, tethered, and provide only low fidelity feedback. A particularly challenging type of wearable human-machine interface is feel-through haptics: ultra-thin wearables so soft as to be mechanically imperceptible when turned off, yet generating sufficient force when actuated to make virtual objects feel tangible, or to change the perceived texture of a physical object. Here, 18 μm thick soft dielectric elastomer actuators (DEA), directly applied on the skin, reports rich vibrotactile feedback generation from 1 Hz to 500 Hz. Users correctly identifies different frequency and sequence patterns with success rates from 73 to 97% for devices applied on their fingertips. An untethered version weighing only 1.3 grams allowed blindfolded users to correctly identify letters by “seeing” them through their fingers. The silicone-based DEA membrane is mechanically transparent, enabling wearable haptics for the many applications where hand dexterity is critical. The feel-through DEA can be placed in array format anywhere on the body.

an intuitive and immersive sense of an object. Yet in the physical world, nearly everything we accomplish with our hands is based on the rich set of information we gain from our sense of touch.

Haptic devices apply stimuli to the body to convey tactile information. One generally distinguishes between kinesthetic and cutaneous (or tactile) haptics.^[1] The former deals with feeling and controlling of angular position, forces, and torques on joints, while the latter is related to the sensation of touch on the skin, such as skin stretch or vibrations. The forces required for arm or body kinesthetic haptics are orders of magnitude higher than for cutaneous haptics, as the human body can easily generate hundreds of Newton of force, yet we can sense μN of force on our skin. In view of the forces needed, kinesthetic force feedback generally uses pneumatic actuators or electromagnetic motors.^[2–4]

1. Introduction

In augmented reality (AR) and virtual reality (VR) applications, head-mounted displays let us see and hear the virtual or augmented world in high resolution. The sense of touch is however underexplored and underused in these scenarios, despite its great importance for a broad range of daily tasks and applications. Physical interaction with virtual objects currently relies on cumbersome handheld controllers, which cannot provide

For wearable cutaneous haptics, a major challenge for actuators and for control is generating the rich diversity of forces one can feel: we can sense both shear and normal forces from DC up to over 800 Hz^[5,6] and distinguish pinprick with accuracy ranging from mm on fingertips^[7] to several cms on the back.^[8] Single vibrating motors or piezoelectric based buzzers are widely used in consumer electronics (e.g., smartphone, fitness monitors, and smart watches), but provide only very limited information, as they offer only a single frequency and amplitude, and are too rigid for comfortable integration in clothing. Far more sophisticated wearable devices have been developed in research labs, applying skin deformation using normal or shear forces with a range of different technologies.^[9]

Rather than being bulky or stiff, wearable haptics should ideally be mechanically imperceptible when off, to allow the user to interact with and feel: i) real objects, ii) virtual ones, and iii) haptically augmented objects in tactile AR scenarios,^[10–12] in which real objects are endowed with additional virtual physical properties. For this last case, the user manipulates real objects (e.g., a coffee cup or a paintbrush), but now the tactile feeling of those objects can be dynamically changed. For instance, faces a smooth cube can be made to feel rough or bumpy as the situation evolves, or keys on a keyboard can feel like different patterns are embossed on them. Condino et al. have shown how tactile AR could be used for artery palpation in surgery

Dr. X. Ji, Dr. V. Cacucciolo, Prof. H. Shea
Soft Transducers Laboratory (LMTS)
École Polytechnique Fédérale de Lausanne (EPFL)
Rue de la Maladière 71B, Neuchâtel 2000, Switzerland
E-mail: herbert.shea@epfl.ch

Dr. X. Liu, Dr. Y. Civet, Prof. Y. Perriard
Integrated Actuators Laboratory (LAI)
École Polytechnique Fédérale de Lausanne (EPFL)
Rue de la Maladière 71B, Neuchâtel 2000, Switzerland

Dr. A. El Haitami, Prof. S. Cantin
Laboratoire de Physicochimie des Polymères et des Interfaces (LPPI)
Université de Cergy-Pontoise
5 mail Gay Lussac, Cergy-Pontoise Cedex 95031, France

 The ORCID identification number(s) for the author(s) of this article can be found under <https://doi.org/10.1002/adfm.202006639>.

DOI: 10.1002/adfm.202006639

training,^[13] and Whithana et al. added localized dynamically changing tactile properties of 3D objects such as model cars for an enhanced design process.^[11]

Given the importance of hand for manipulation and the associate high density of mechanoreceptors in fingertips, we focus here on wearable haptics for the hand. The ultimate cutaneous device for the hand would locally stimulate the skin to simulate surface texture, and stretch and push on the skin to simulate external forces, yet be as imperceptible as a tattoo, allowing unencumbered interaction with the environment, retaining normal sensation and grasping ability. One non-mechanical solution is electro-tactile (or electro-stimulation) devices, that operate by driving current through the skin, thus electrically exciting mechanoreceptors, giving the user the impression of feeling a vibration where the current passes.^[14–16] Tactoo^[11] is an electro-tactile feel-through device, 35 μm thick, in appearance similar to a temporary tattoo. It contains a matrix of silver electrodes in contact with the skin, can be applied to fingertips and forearm, and allows for localized haptic notification while touching objects. The device delivers a limited range of sensation akin to buzzing.

Direct mechanical stimulation of the skin could provide more immersive and realistic haptic sensations than electrostimulation. Yet until now soft actuators able to provide enough force and displacement for haptic perception, while being mechanically transparent, remains an open challenge. Soft actuators that can supply sufficient force for haptics are widespread, but making such devices only a few tens of microns thick (so that they are mechanically imperceptible when off) requires extremely high power density and an actuation principle compatible with ultra-thin layers. For example, even pneumatic actuation with 100 μm wide channels is too thick to be mechanically transparent.

The displacement and force needed to reach perception threshold is a central issue for haptics devices, and cannot be defined with a single pair of values. The mechanical stimulus threshold depends on many factors, beyond actuation frequency, including taxel (a taxel is the mechanical analogue of a pixel) area, stiffness (e.g., hard pin versus soft button), position on the body, gender, age, skin condition, haptic training, presence of other non-tactile stimuli, etc.^[5,6] Testing on human subjects is nearly always required to validate the haptic effectiveness.

Absolute thresholds vary significantly across the literature. Representative values for absolute thresholds of tactile perception on glabrous skin of the hand include 30 μm displacement on the thenar eminence (base of thumb),^[17] and a force threshold of 10 mN at 5 Hz and 10 Hz on the index finger.^[18] For a dielectric elastomer actuator (DEA) taxel, a detection threshold of 27 mN for force and 200 μm for displacement was reported at 1 Hz excitation frequency, while at 10 Hz these values decrease to 4 mN and 30 μm .^[19] The tactile perception threshold for less sensitive parts of the body can be more than an order of magnitude higher than for fingertips. For example, Nittala et al. report tactile sensitivity of 0.04 g for fingertip, but 0.64 g for the hand and 0.9 g for the forearm.^[7] A comprehensive review can be found in refs. [5,20].

The mechanical stimuli on fingertips can be generated using a number of portable methods including:^[9] electromagnetic

motors,^[21–23] electromagnetic actuators,^[24,25] shape memory polymers,^[26] piezoelectric actuators,^[27] pneumatic actuators,^[28–30] DEAs,^[19,31–36] and electrostatic zipping.^[37] Many compliant actuators developed for soft robotics are relevant for wearable haptics.^[38] Commercially available gloves incorporating tactile feedback rely on vibrotactile sensations from either eccentric-mass motors or from piezoelectrically driven vibrating masses, offering essentially simple buzzing.^[39] Microfluidic and pneumatically driven systems have been announced,^[30,40] but require a compressor, making untethered operation impractical.

Motor-based devices enable high shear and normal forces, but are bulky and contain rigid elements such as motor casings and gears that prevent integration in clothing. In contrast, elastomer and electroactive polymer-based solutions are compliant, allowing for easy shape matching to the fingertip or other body parts. The mechanical impedance of soft actuators is a natural match to the skin.^[37] Silicone elastomers can be made compliant and thin enough to allow using one's sense of touch while wearing silicone patches on fingertips.^[7]

DEAs are particularly suitable candidates for haptics on fingertips: they are intrinsically thin (typically under 100 μm),^[41] can respond up to several kHz,^[42] provide large actuation strain,^[43] have MPa range stiffness, and scale down favorably.^[44] DEAs are electrically controlled, and can be completely silent, requiring no pumps or gears, making them particularly suited for on-body haptics.^[45]

DEAs-based wearable haptic devices have relied to date on an out-of-plane motion to deform the skin.^[19,31–33] One approach uses hydrostatic coupling between the DEA active membrane and a passive membrane that is in contact with the skin.^[19,31,32] When the DEA membrane is activated, the pressure applied to the skin by the passive membrane changes. In another approach, the DEA active membrane buckles when activated,^[33,36] requiring a gap between the DEA and the skin, so that the DEA membrane touches the skin when on, but not when off. For both configurations the air or liquid gap between the DEA and the skin prevents feeling objects through the devices. Larger and more powerful DEAs have been mounted on the forearm for haptic communication,^[45] but also are not compatible with feeling objects through the actuator.

Most wearable haptic devices are wired, an obvious obstacle to many mobile applications. Although untethered haptic devices have been developed, their form factor makes them unsuitable for the fingertip use or impairs the normal use of the fingertip or even of the entire hand.

Addressing the above-mentioned challenges on mechanically transparent haptic actuators, we report feel-through low-voltage DEAs (FT-DEAs), shown in **Figure 1**, which we demonstrate on fingertips. The ultrasoft FT-DEAs remain in intimate contact with the glabrous fingertip skin even while handling an object. FT-DEAs are based on recently reported ultra-thin low-voltage DEAs.^[46] The extremely low thickness of these actuators (18 μm for three active layers) is what enables the mechanoreceptors covered by the thin membrane to remain sensitive to external stimuli.^[7] With its negligible weight (1 mg), the thin membrane allows unfettered use of the fingertips and fine sensation (e.g., holding a pen, using touch

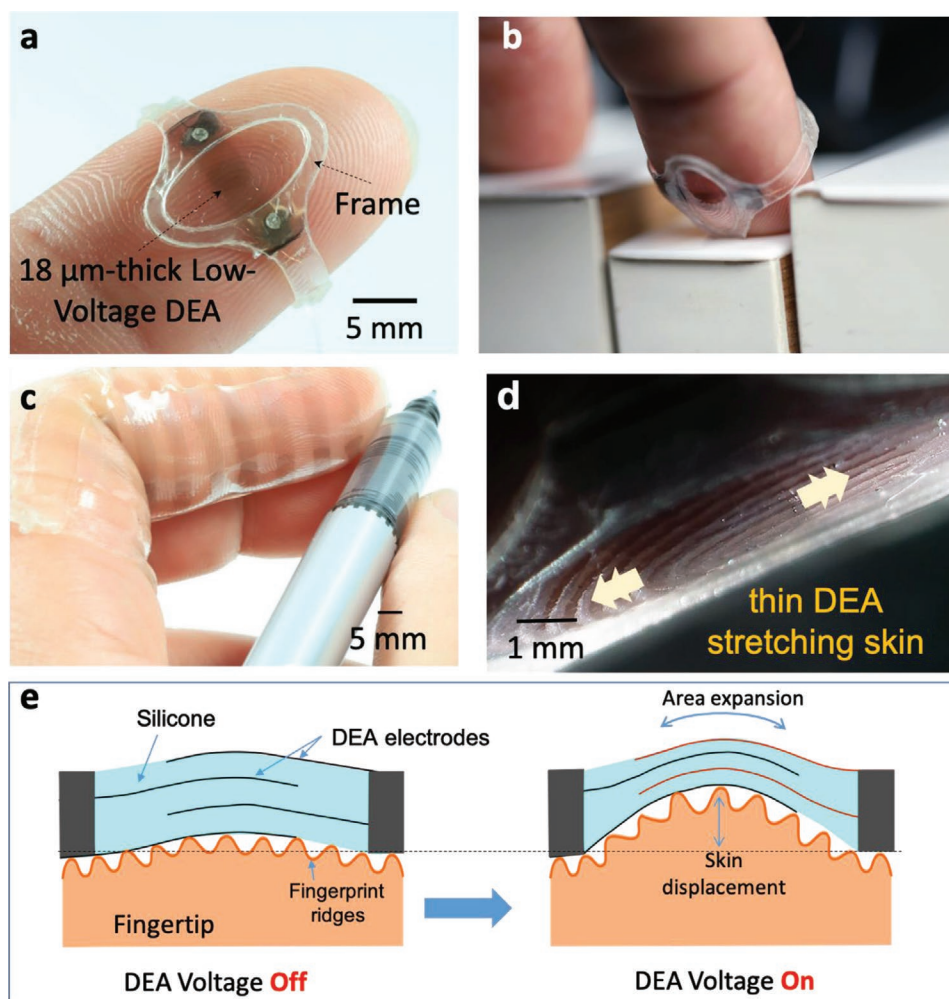


Figure 1. Feel-through DEAs (FT-DEAs) haptic device. a) Photo of FT-DEA on a fingertip, b) Playing the piano while wearing a FT-DEA, c) array of 10 frameless FT-DEAs on a finger. d) fingertip ridges stretched by the devices (see Movie S1, Supporting Information, showing 1 Hz fingerprint motion due to FT-DEA). e) schematic cross-section showing DEA in-plane expansion due to electrostatic forces when a voltage is applied, gently stretching the skin to provide haptic feedback.

screen, touch typing etc.). At the same time, the power density of these 18 μm -thick actuators is so large (over 10^6 W m^{-3} at 580-Hz resonance^[46]) that they can generate force and displacement well above the sensation threshold. The active thin membrane can generate on-demand highly localized and rich haptic feedback signals by gently deforming the skin with frequencies from 1 Hz up to 500 Hz. The “feel-through” device is mechanically transparent, even when active, allowing it to be worn when performing other tasks. Thanks to the low operating voltage of our DEAs, we integrated electronics and power supply on package mounted on a fingernail, enabling an untethered version of this device including photodiodes for autonomous determination of what haptic signal to generate. With its rechargeable battery, the electronics weigh 1.3 g. We show that a blind-folded user equipped with an autonomous FT-DEA could “see” printed letters using his finger. These autonomous, mechanically transparent “feel-through” devices bring new possibilities for the next generation of wearable human-machine interfaces.

2. Results and Discussion

2.1. Operating Principle of the “Feel-through” Haptic Device

The “feel-through” DEA device is a multi-layer DEA, consisting of stacked nm-thick electrodes and μm -thick elastomer films. The ground and actuated electrodes overlap in a central 3 mm diameter active zone. Adapting the method we reported for a DEA-driven insect robot,^[46] each DEA layer consists of a 6 μm -thick polydimethylsiloxane (PDMS) dielectric membrane enclosed between two nm-thick electrodes made of single-walled carbon nanotube (SWCNT) fabricated using the Langmuir–Schaefer method.^[47] The total thickness of the stacked FT-DEA structure is 18 μm . The fabrication steps are shown in Figure S1, Supporting Information. The active membrane is directly in contact with the fingertip in a “feel-through” configuration, meaning that the device is mechanically transparent, leaving the finger free to move and able to directly feel objects.

Silicone elastomers were used as the dielectric membrane for the DEA rather than acrylics such as VHB because of silicone's low loss tangent, demonstrated high speed operation in DEA,^[42] ease of processing,^[48] commercial availability in thin films, biocompatibility,^[49] and very low adhesion compared to acrylics, allowing the FT-DEA to be repositioned multiple times on the skin.

Electrodes are a major technological challenge for DEAs with very thin membranes.^[47,50] While using thin (e.g., less than 10 μm thick) elastomer membranes allows operating DEAs at electric fields near dielectric breakdown using voltages well below 1 kV, two main problems appear: i) the relative stiffening impact of the electrodes becomes more important, and ii) a thinner DEA has higher capacitance, leading to longer RC time constants. Thin and stretchable electrodes generally have high sheet resistance.^[51,52] By using amphiphilic SWCNTs spread and organized at the air-water interface in a Langmuir trough, we obtain a several nm-thick SWCNT carpet that acts as electrodes after Langmuir-Schaefer transfer onto the dielectric membrane. These electrodes add nearly negligible stiffness to the elastomer, and have a low enough resistance to allow operation at several hundred Hz.^[46]

Two versions of FT haptic devices are presented here (Figure 1). The first version uses a flexible frame (Figure 1a,b) to maintain the DEA pre-stretch and to facilitate the electrical connection between the DEA electrodes and very thin wires. The frame has an oval shape with internal dimension of 6 mm x 12 mm, surrounding the circular DEA. The second version has no frame (Figure 1c), making it entirely stretchable. It is attached to the body using a skin-compatible adhesive. The finger then effectively serves as the frame. These frameless devices are meant for single use because the 18 μm -thick DEA can be damaged when peeled off. The devices with a frame are more robust and can be mounted and removed multiple times. In both cases, the ground electrode is in contact with the skin.

The FT-DEAs stretch the skin to generate feedback (Figure 1d and Movie S1, Supporting Information). The operating principle is schematically presented in Figure 1e. The thin elastomer membrane very gently compresses the skin when the DEA is off (Figure 1e left). The stretch is low enough that users do not feel any mechanical constraint when the device is off. When the DEA is turned on, the surface area of the elastomer increases while its thickness decreases, both stretching the skin and allowing it to move in the direction normal to the DEA plane (Figure 1e right). The FT-DEA can be operated at frequencies from 1 to 500 Hz to generate rich haptic information. Movie S1, Supporting Information, shows fingerprint ridges being stretched by the DEA at 1 Hz. Due to the RC time constant of the DEA, approximately 2 ms, and more importantly to mechanical damping, the highest frequency we operated at the body was 500 Hz. The FT-DEA device also operates well at DC, providing a static skin stretch.

2.2. FT-DEA Strain Characterization

The FT-DEA devices with frames were first characterized on a test bench to determine unloaded strain versus voltage and frequency response. Area strain of the FT-DEA is plotted as a

function of applied DC voltage in Figure 2a. The device reaches over 25% in-plane area strain at 450 V. This drive voltage is roughly an order of magnitude lower than for most DEAs, thanks to the use of thin elastomer layers, and to the highly compliant carbon nanotube-based electrodes.^[46] The 6 μm

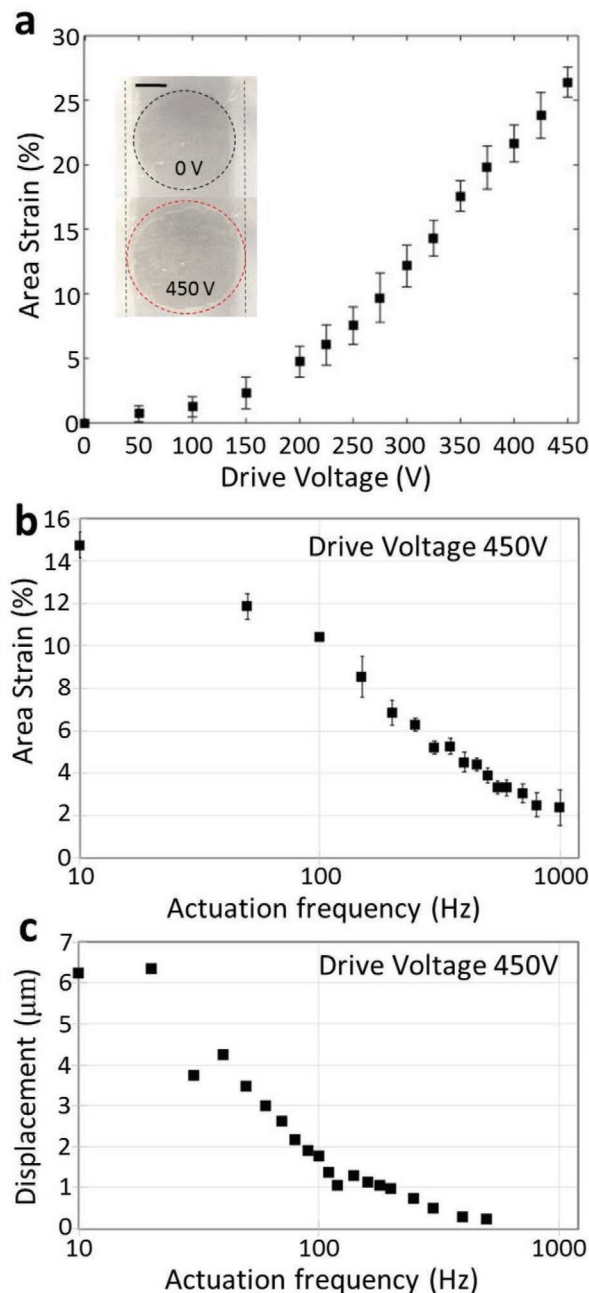


Figure 2. a) Area strain of a free-standing 3 mm-diameter circular FT-DEA as a function of the applied voltage. Scale bar 1 mm for inset photos at 0V and at 450 V. The error bars correspond to the standard deviation of 5 measurements taken on the same sample. b) Area strain of a free-standing FT-DEA at 450 V versus driving frequency. The error bars correspond to standard deviations from 5 measurements. c) Out-of-plane displacement of the skin as a function of the drive frequency when deformed by a FT-DEA.

thick dielectric layer allows obtaining an electric field near the approximately $75 \text{ V } \mu\text{m}^{-1}$ breakdown field for Silbione LSR4305 silicone elastomer at 450 V in ambient conditions.^[53] The few nanometer thick SWCNT-based electrodes provide the very low stiffness needed for high strain and the good electrical conductivity required for high-speed operation. The “low-voltage”, compared to typical DEAs, is what enables the very low mass electronics used for an untethered version, described later.

Figure 2b plots the FT-DEA area strain versus actuation frequency at a voltage of 450V. The strain is 14% at 10 Hz (see Figure S2, Supporting Information). With increasing frequency, the actuation strain decreases mostly due to the viscoelasticity of the soft silicone that was used. The RC time constant of the FT-DEA gives a cutoff frequency of about 430 Hz.

The out-of-plane response of FT-DEA was then characterized for a device with a frame mounted on a fingertip, using a laser Doppler vibrometer (see Experimental Section). Figure 2c plots out-of-plane (i.e., normal) displacement of the skin as a function of the DEA actuation frequency for a fixed drive amplitude of 450 V. $6 \mu\text{m}$ of motion is observed for low frequencies, with an amplitude that decreases with increasing frequency, with a slope higher than for the off-finger characterization (Figure 2b), probably due to the added mechanical damping from the finger. While the data on unmounted FT-DEA devices are highly repeatable, the motion amplitude measured on fingers depends on fingertip mechanical properties (which vary from finger to finger) and on mounting method.

The force on the finger skin can be estimated from the measured strain, materials properties, and geometry. For 10% area strain, that is, the strain seen at 10 Hz, the on-skin force is approximately 9 mN. This is of the same magnitude as reported perception thresholds for devices for which the user presses his finger on an actuator.

2.3. Haptic User Tests with FT-DEA on Fingertip

Given the unique mechanical configuration of the FT-DEA where an extremely soft elastomer actuator is mounted directly on the skin, we explored how users perceive different signals from the $18 \mu\text{m}$ thick FT-DEA.

Qualitatively, when wearing the device on a fingertip, users report that low frequency (1 to 20 Hz) actuation feels like well-localized pulsing, with the motion felt precisely at the DEA location. For higher frequency actuation (100 to 500 Hz) users report feeling vibration sensation over the entire fingertip. This localization agrees well with literature and with the understanding of the different types of mechanoreceptors in our glabrous skin, with Merkel disks providing high spatial resolution for low-frequency stimuli, and Ruffini corpuscles and Pacinian corpuscles providing lower resolution but responding to higher frequencies.^[6,54]

For quantitative tests, we recruited 14 untrained, healthy volunteers (7 females and 7 males, ranging in age from 27 to 46 years old). They wore an FT-DEA haptic device on their left index fingertip, see Figure S3, Supporting Information. We performed two series of tests on each volunteer. Test 1 measures the signal intensity perceived by the users as a function of the FT-DEA actuation frequency for a square wave. Test 2 is

signal identification study: users are randomly shown one of 6 different waveforms, and are asked to identify the waveform. Complete data sets were obtained for 11 of the 14 users.

The perception results for Test 1 from 1 to 500 Hz are shown in Figure 3a, averaged over all 11 users. The drive voltage was between 420 and 440 V, adapted to provide the same electric field for all FT-DEAs. The vertical axis is a perception scale; the user was asked to rate the sensation using the following scale: 0: no feeling, 1: difficult to feel, 2: can be felt, 3: can be felt easily, 4: can be felt very easily. The randomization process for the 120 stimuli (10 times the 11 frequencies and “off” state) applied for each user and experimental procedure is described in the Experimental section.

Nearly all users easily feel all frequencies, with higher reported sensation for frequencies between 10 and 200 Hz. Higher and lower frequencies are felt less strongly. Users correctly identify when no voltage was applied. Test 1 showed that FT-DEA devices can generate signals that are well above the perception threshold. There is a significant user to user variability, as can be seen in Figure S4, Supporting Information, in which the data for all 11 subjects are shown. Some users have lower sensation at higher frequencies.

Test 2 measures how users can differentiate complex notification signals. The waveforms are shown in Figure S5, Supporting Information. Each signal duration is 6 s. In view of the results from test 1 that showed users could feel a broad frequency range, the signals were chosen to include low frequencies, which feels like gentle tapping, and higher frequencies, where one perceives a vibrotactile response. Signal 1 is a 10 Hz square wave. Signal 2 is a 200 Hz square wave. Signal 3 alternates between 10 and 200 Hz every 1 s. Signals 4 and 5 are frequency sweeps from DC to 200 Hz and from 200 Hz to DC, with a frequency step every second. Signal 6 has the voltage set to zero to verify that users can tell when the devices are not actuated.

Figure 3b shows the confusion matrix based on the average performance on all the 11 volunteers. Rows correspond to the applied signal. Columns indicate the signal identified by the user. Correct identified signals lie on the diagonal of the matrix. Users correctly distinguish whether the device is on or off (Signal 6) with an Identification Rate (IR) of 97%. For signals 1, 2, and 3, the users have an IR of over 85%. For the more complex signals 4 and 5, the IR is above 70%. Random guessing would lead to an IR of only 20%. The confusion matrix corresponding to all subjects is shown in Figure S6, Supporting Information.

The confusion matrix demonstrates that the “feel-through” devices are effective at delivering rich on-body notifications at different operating frequencies, including feedback signals with different intensities and frequencies.

In unquantified tests, neither the authors nor the test subjects noticed any decrease in tactile perception when handling everyday objects when wearing the FT-DEA device. Given the $18 \mu\text{m}$ thickness and the low Young's modulus of the silicone, this is well in line with a detailed study exploring how epidermal devices affect tactile perception by Nitala et al.^[7] They performed perception studies with silicone patches worn on fingertips, hand, and forearm for patches of three different stiffnesses, with flexural rigidities of 2×10^{-9} , 1.3×10^{-7} , and

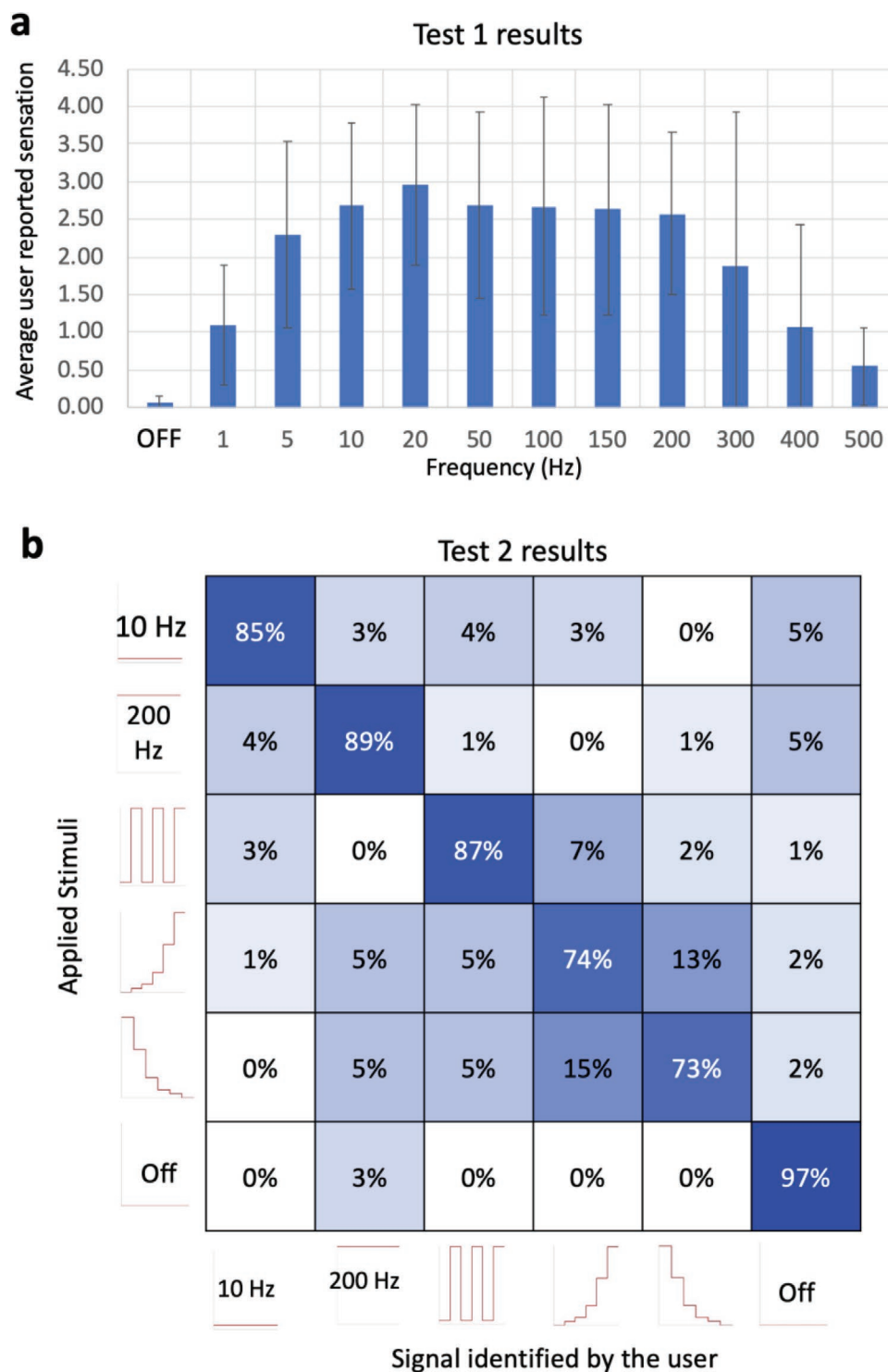


Figure 3. a) Outcome of haptic test 1, showing average user reported feeling (scale 0–4) versus frequency for a square wave for feel-through device worn on an index finger, as in Figure 1a. See Figure S3, Supporting Information, for test setup details. The error bars are the standard deviations from the 11 users. b) Outcome of haptic test 2: Confusion matrix showing the average response of 11 untrained volunteers to the 6 stimuli signals delivered to a single wired FT-DEA mounted on the left index fingertip. A very high correct identification rate is observed, validating a range of notification scenarios.

1.2×10^{-5} Nm. For their softest patch, compared to bare skin, Nittala et al. report a 6% increase for two-point orientation discrimination, an increase of 30% for tactile sensitivity threshold and a

34% increase in surface offset threshold for tactile discrimination of textured surfaces. Importantly these average increases for patch versus bare skin are all smaller than the measurement uncertainty

in the thresholds. Our FT-DEA device has a flexural rigidity of only $6 \cdot 10^{-10}$ Nm, half the value of their softest patch, which is why we consider it to be imperceptible when off.

2.4. Demonstration of a Haptic Reader

The devices used in haptic Test 1 and Test 2 were connected to a table-top power supply using ultra-thin wires (barely visible in Figure 1a,b). In this section, we demonstrate a use-case of the haptic device in an untethered scenario (Figure 4), where the FT-DEA allows a blind-folded user to feel if his finger is over a white or a black surface, and thus by moving his finger to identify letters under a smooth plastic sheet.

The FT-DEA device is integrated with compact lightweight (1.3 g) on-board electronics, including battery, microcontroller, and photodiodes (Figure 4a,b). The electronics are a modified version of the electronics we developed for an untethered DEA-driven soft robotic insect, but with only 1 channel and a form-factor suited for wrapping around a finger.^[46] The drive electronics can output a voltage of up to 480 V at a frequency up to 1 kHz. The on-board battery allows for continuous operation of over 30 min on one charge. The low mass and low volume are possible thanks to the sub-500 V drive voltage of the DEA. The photodiodes here serve not for robot navigation as in ref. [46], but are used to detect if the fingertip is held over black ink or over white paper.

We programmed the micro-controller to provide vibrotactile feedback based on the input from the two photodiodes.

As shown schematically in Figure 4c top, the FT-DEA is off when the photodiodes are near a white surface. When held over a black surface, the FT-DEA is actuated at 200 Hz at 420 V (Figure 4c bottom).

To demonstrate the operation of the untethered FT-DEA, the letters E, P, F, and L (dimension: 5 cm × 10 cm) are printed using a laser-printer on office paper. The four letters are randomly placed and oriented, then covered with a flat transparent 1 mm-thick acrylic plate. Wearing the wireless FT-DEA haptic device on his left-hand index fingertip (Figure 4d), the blindfolded user freely scans his finger over the smooth plastic plate. Based on the feedback signals received from the FT-DEA device, the user correctly identifies both the position and orientation of all the letters (see Movie S2, Supporting Information). This augmented perception allows the user to replace the sense of sight by the sense of touch, turning a smooth surface into an active one.

Using the device shown in Figure 4 approximately 5 mm wide lines could be perceived. The resolution depends on several factors including how fast the finger is moved, how high above the image the finger is placed, and photodiode optics and placement.

3. Conclusion

We developed an untethered, wearable haptic device that generates rich vibrotactile feedback on the fingertip, but that could be applied anywhere on the body (e.g., Figure 1c). The active part is a DEA that adheres to the fingertip and

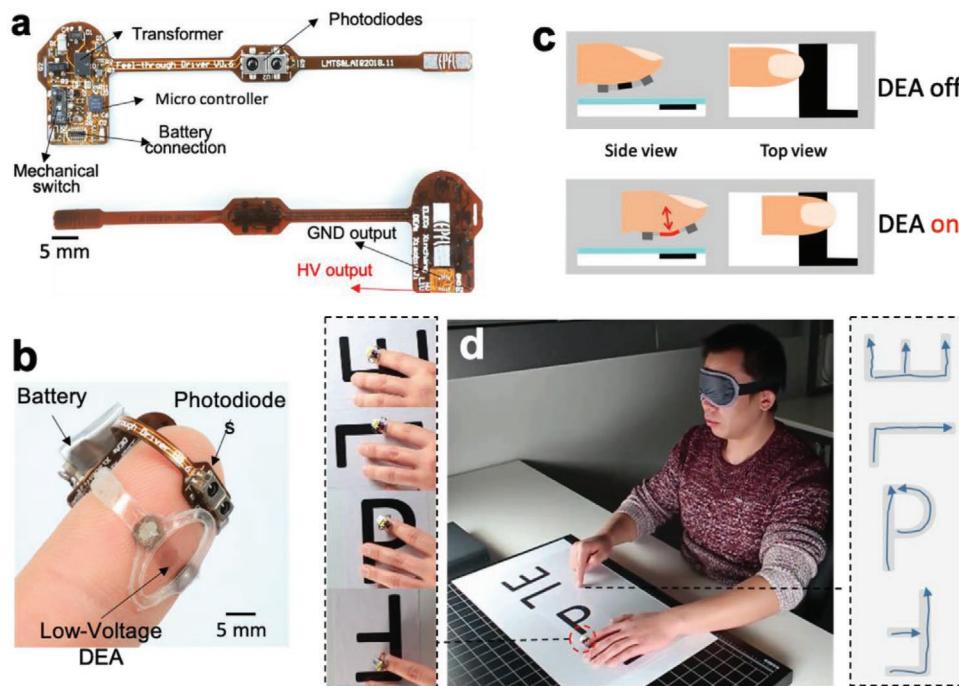


Figure 4. Untethered FT-DEA for wireless feel-through haptics. a) Photo of the wireless driver circuit (mass 1.3 g). b) Photo of untethered “feel-through” haptic device on a fingertip, with integrated electronics and rechargeable battery. Here the photodiodes face out from the fingertip, to enable the “seeing with fingertips”. c) Operating principle: the FT-DEA is off if the photodiodes are over a white surface. The FT-DEA vibrates at 200 Hz when the photodiodes are over a dark surface. d) The blindfolded user correctly identifies randomly rotated and placed letters E, P, F, and L. The feel-through device thus allows users to “see” with his/her fingertip (see Movie S2, Supporting Information).

gently stretches and compresses it at frequencies from 1 to 500 Hz. Thanks to its very low thickness (18 μm) and use of soft elastomers, the active membrane is mechanically transparent, letting the user “feel-through” the device. The untethered version, including actuator, electronics, and battery has a total weight of 1.3 g, making it comfortable to wear for extended periods during everyday activities. The devices reported here generate sufficient force for easy perception on fingertips and on the face. Obtaining readily discernible forces when mounted elsewhere on the body would require stacking more layers or using larger area DEAs to increase the force.

We characterized the electro-mechanical response of the device at different frequencies both off-finger and on-finger, demonstrating its ability to deform the skin in normal direction by over 6 μm . Haptic tests conducted on 11 volunteers quantified the ability of the FT-DEA device to provide rich vibrotactile haptic signals. Five different signals with different frequency profiles were correctly identified with rates ranging from 73 to 97%.

We demonstrated the wireless FT-DEA in a tactile reading scenario. Wearing the FT-DEA device, a blindfolded user used his index finger to “see” randomly oriented black letters on white background. The FT-DEA could also enable the wearer to use his fingertip to “see” colors by adding color filters on front of the photodiodes, or by using a small color camera. Going further by integrating different types of sensors (e.g., microphone, ultrasound distance sensor, gas sensor), the FT-DEA device could enable users to use their sense of touch as augmented perception to perceive sound, 3D space and smell.

The “feel-through” haptic devices can be used for mixed and AR scenarios, and allow users to feel virtual objects in VR. The “feel-through” haptic device represents a new form of human-machine interface, one that provides haptic feedback while being mechanically transparent and nearly imperceptible when turned off. The user holds and uses real objects, instruments, and tools in an unencumbered manner, yet can receive highly localized tactile information, allowing for feeling different surface textures or vibrations depending on the AR context. The objects are not changed, but how the user feels them is dynamically changed, for example, a silicone tube can feel like it is pulsing for surgical simulation,^[13] or a tennis player can be made to feel that the handle is not ideally gripped. “Feel-through” haptics enables the use of on-finger haptics in the wide range of applications where the hand dexterity is critical, such as painting, surgery and playing musical instruments.

4. Experimental Section

FT-DEA Fabrication and Assembly: The fabrication process of the low-voltage DEA in the “feel-through” device was based on the process developed by the authors for DEA to drive an untethered soft crawling robot,^[46] but adapted here for the higher compliance for mounting on a finger, and without the robot leg. The fabrication process for the “feel-through” device (Figure 1a) is: Silbione LSR 4305 parts A and B are mixed with OS-2 (Dow Corning) solvent as described in ref. [48] in mass fractions of 25 wt%, 25 wt%, and 50 wt% using a planetary mixer (Thinky, ARE-250). A 23 μm -thick PDMS membrane was fabricated by casting the uncured PDMS on a Polyethylene terephthalate (PET) substrate coated with a Polyacrylic acid (PAA) sacrificial layer, using an automatic film applicator (Zehntner) with a blade gap of 100 μm . A suspended PDMS membrane was then obtained by dissolving the PAA

sacrificial layer in hot water. The 23 μm -thick PDMS membrane was equi-biaxially pre-stretched (to a ratio of 1.8) to a thickness of 6.5 μm (Figure S1a, Supporting Information), and the prestretch was held by a poly methyl methacrylate (PMMA) holder. These pre-stretched PDMS membranes form the dielectric layers of the stacked DEAs.

Octadecylamine-functionalized SWCNT electrodes were fabricated using the Langmuir-Schaefer (LS) method,^[47] using a mask to define the electrode shape once transferred on the PDMS substrate. The PDMS was treated by Oxygen Plasma (OP) to enhance the quality of the electrode transfer. A second sacrificial mask with the same pattern as the mask for the LS transfer was overlapped on the first one before the OP treatment. The second mask prevents OP treatment on the first mask. After the OP treatment (Diener, ZEPTO) at 30 W power for 6 s, the second mask was peeled off (Figure S1b, Supporting Information) and the SWCNTs electrodes were transferred. By peeling of the first mask, a suspended PDMS with patterned SWCNTs electrodes was obtained (Figure S1c, Supporting Information). The masks were laser-cut (Trotec, Speedy 300) from 50 μm -thick Polyester sheets.

For robust electrical contacts to the thin CNT electrodes, a 20 nm-thick gold layer was sputtered on the LS transferred electrodes, 3 mm away from the DEA active region (Figure S1d, Supporting Information). The masks for gold patterning were made from laser-cut paper. A 1 mm space gap between the mask and the pre-stretched PDMS membrane was used to avoid direct contact between the two. After the gold layer deposition, the PDMS layer with an electrode on one side was ready for stacking. The above processes were repeated (from Figure S1a to S1d, Supporting Information) three times, to have three PDMS membranes each with an electrode on one side. One membrane was flipped over in order to apply the second electrode on the backside of that PDMS membrane. This handling process was done as in ref. [47] by using PDMS membrane holders of different sizes. The stacked DEA was assembled on a flexible 125 μm -thick PET frame (Figure S1g, Supporting Information). Silicone adhesive was used to bond together the PDMS layers. Conductive silver epoxy was applied on each patterned gold layer for electrical conductivity. Thin copper wires were connected to the assembly by forcing them into holes on the frame and bonding them with conductive silver epoxy (Figure S1g, Supporting Information). The final assembled stacked layers were vacuum treated for 10 min to remove any small air bubbles from the lamination step. After degassing, the stacked layers were placed in an oven at 80 °C for 2 h to cure the conductive silver epoxy. The curing step completes the fabrication of the stacked DEAs. For the wearable “feel-through” devices, the holders were used to both shield the connecting wires of the stacked DEA and mechanically hold the device on the fingertip.

For the fabrication of the “feel-through” device without frame (Figure 1c), the steps were the same as the ones described above, but using different geometries for the pre-stretched PDMS membrane holders and for the masks. Skin-compatible double-sided adhesive was used to attach the PDMS membranes on the finger skin.

Control Electronics: The 1.3 g electronic circuit was similar to the power supply implemented to drive the DEAnsect untethered soft robot^[46] but with only one channel. An open-loop flyback circuit was used to generate, after design optimization, a 480 V output voltage (HV). A MOSFET was used to discharge the DEA. By alternating these two operations (charging/discharging), the actuator can be driven at the desired frequency.

The on-board control algorithm has been pre-calibrated as a function of the battery voltage to maintain a stable HV output and, at the same time, keep the system operating at the highest efficiency point so that the operating time can be maximized. The on-board battery allows for continuous operation for over 30 min on one charge.

The Flexible Printed Board (FPB) was designed to be portable and easily mounted and removed from fingers of different sizes (Figure 4a). The main electrical components were placed only on the top side (10 mm x 18 mm). A reinforcement layer has been added on the bottom side of the FPB to improve the rigidity, and was used as an insulating layer between the finger/FT-DEA and the circuit. A rather large infrared

module has been adopted allowing to sense distances up to 10 mm in order to adapt the finger-feeling application. A robust switch and additional LEDs were included to facilitate the user interaction with the driver.

Testing Methodology for Haptic Perception on Volunteers: The user sits in front of a table in a quiet room, and places his/her left arm on the table with the left hand on a soft support (Figure S3, Supporting Information) so that the user remains comfortable during testing. A computer is in front of the volunteer, who can use his/her right-hand to press keys. Users cannot hear or see any changes in the drive electronics that might give an indication of the applied haptic signal. The FT-DEA was mounted on the left index finger. For each volunteer, testing was carried out in two parts:

Test 1: Perceived Signal Intensity Test as a Function of Frequency: The aim of this experiment was to study the perceived intensity of the feedback given by the FT-DEA operating at different frequencies.

The actuation voltage value was adjusted on each device (420 to 440 V) to obtain the same strain, compensating for variations in the fabrication process.

A graphical interface was displayed on the screen. When the user was ready for the testing, the user clicks “start experiment”. A random signal from the above 12 signals (zero volts or full voltage at 1, 5, 10, 20, 50, 100, 150, 200, 300, 400, or 500 Hz) was applied to the device. The user waits at least 2 s, then types a number from 0 to 4, corresponding to the perceived signal intensity as:

- 0: I do not feel any motion
- 1: difficult to feel
- 2: can be felt
- 3: can be felt easily
- 4: can be felt very easily

Once the user was ready to feel another signal, they press the “Enter” key. Each of the 12 different signals were applied randomly 10 times (in total 120 signals for testing, taking typically about 15 min to complete the whole session for one user).

Test2: Signal Identification Study: The aim of this experiment was to study how users distinguish and recognize different signals generated by the FT-DEA. Six different predefined signals (Figure S5, Supporting Information) were used in this experiment. There were two steps: a) a learning stage where the user became familiar with the six signals, and b) a recognition stage when the user was asked to identify randomly displayed signals.

A testing interface was displayed on a computer display. When the user was ready to begin the learning stage, they click “start learning”. By then pressing a number from 1 to 6, the corresponding signal was sent to the haptic device, with the signal number displayed on the computer screen. The users practice freely as long as they wish. An information sheet with the graphical waveform of the 6 signals was available to help users remember the signals.

Once the user was ready, they stop learning by clicking “Abort learning” and start the recognition experiment by clicking “Start Experiment”. A random signal from the predefined set was sent to the haptic device. The user feels the signal for at least 6 s, then inputs the number corresponding to the identified signal. Once the user was ready to continue, they press the “enter” key to start the next signal. Users can take short breaks (generally they stop for less than 1 min). Each of the 6 different signals was applied randomly 10 times (in total 60 signals, taking typically about 40 min per user).

The results of the haptic tests are summarized in Figures S4 and S6, Supporting Information.

Comfort: Although mechanically extremely thin, wearing the device continuously for several hours can cause some sweating of the fingertips. Using perforated silicone for all regions except the central DEA region would decrease the sweating and increase long-term wearability.

Safety Considerations: The device was very low power (up to a few mW), and uses very low currents.^[46] User safety was ensured by multiple levels: a) the current of both the fixed and the untethered power supply was limited to 120 μ A, b) the capacitance of the DEA was only 90 pF, meaning it cannot store enough charge to harm a human, c) the ground

electrode was skin facing, d) high quality dielectrics act as excellent insulators.

According to Pourazadi et al.,^[55] a reasonable safety threshold for DEA applications is at 20 mA continuous DC current and >100 nF total capacitance. The FT-DEA was several orders of magnitude below these metrics.

The electric fields from the DEA that might enter the human body were only due to fringing fields at the periphery of the DEA. Given the 6 μ m dielectric thickness, significant electric fields will extend by at most a few tens μ m from the side of the DEA, that is, only in top layers of the epidermis.

Supporting Information

Supporting Information is available from the Wiley Online Library or from the author.

Acknowledgements

The authors thank Dr. J. Zarate for advice on haptic testing and Dr. E. Leroy for the Python programming. This work was funded by the European Union’s Horizon 2020 research and innovation program under the Marie Skłodowska-Curie grant agreement No 641822-MICACT via the Swiss State Secretariat for Education, Research, and Innovation, and by the Hasler Foundation Cyber-Human Systems program. The perception studies on human volunteers was approved by the EPFL Human Research Ethics Committee (HREC 047–2018/25.11.2018). Informed consent was obtained from all volunteers.

Conflict of Interest

The authors declare no conflict of interest.

Keywords

dielectric elastomer actuator, haptics, human-machine interface, soft robot, wearable

Received: August 7, 2020

Revised: September 14, 2020

Published online:

- [1] H. Culbertson, S. B. Schorr, A. M. Okamura, *Annu. Rev. Control, Rob., Auton. Syst.* **2018**, *1*, 385.
- [2] P. Polygerinos, Z. Wang, K. C. Galloway, R. J. Wood, C. J. Walsh, *Rob., Auton. Syst.* **2015**, *73*, 135.
- [3] G. Agarwal, M. A. Robertson, H. Sonar, J. Paik, *Sci. Rep.* **2017**, *7*, 14391.
- [4] S. Koizumi, Y. Shimada, T.-H. Chang, H. Nabae, G. Endo, K. Suzumori, M. Mita, K. Saitoh, K. Hatakeyama, S. Chida, in *IEEE/SICE International Symposium on System Integration (SII)*, IEEE, Honolulu, HI, USA **2020**, pp. 93–98.
- [5] C. Hatzfeld, T. A. Kern, *Engineering Haptic Devices*, 2nd ed, Springer, London, **2014**.
- [6] S. Biswas, Y. Visell, *Adv. Mater. Technol.* **2019**, *4*, 1900042.
- [7] A. S. Nittala, K. Kruttwig, J. Lee, R. Bennewitz, E. Arzt, J. Steimle, in *Proc. 2019 CHI Conf. Human Factors in Computing Systems – CHI ’19*, ACM Press, Glasgow, Scotland **2019**, pp. 1–16.

- [8] D. Purves, G. J. Augustine, D. Fitzpatrick, W. C. Hall, A.-S. Lamantia, J. O. Mcnamara, S. M. Williams, *Neuroscience*, Sinauer Associates, Sunderland, MA, USA **2004**.
- [9] C. Pacchierotti, S. Sinclair, M. Solazzi, A. Frisoli, V. Hayward, D. Prattichizzo, *IEEE Trans. Haptics* **2017**, *10*, 580.
- [10] O. Bau, I. Poupyrev, *ACM Trans. Graph.* **2012**, *31*, 89.
- [11] A. Withana, D. Groeger, J. Steimle, in *The 31st Annual ACM Symp. User Interface Software and Technology – UIST '18*, ACM Press, Berlin, Germany **2018**, pp. 365–378.
- [12] T. Murakami, T. Person, C. L. Fernando, K. Minamizawa, in *ACM SIGGRAPH 2017 Posters*, ACM Press, Los Angeles, CA, USA **2017**, pp. 1–2.
- [13] S. Condino, R. M. Vigliani, S. Fani, M. Bianchi, L. Morelli, M. Ferrari, A. Bicchi, V. Ferrari, in *Medical Imaging and Augmented Reality* (Eds: G. Zheng, H. Liao, P. Jannin, P. Cattin, S.-L. Lee), Springer International Publishing, Cham **2016**, pp. 186–197.
- [14] H. Kajimoto, N. Kawakami, T. Maeda, S. Tachi, in *Proc. ICAT, ICAT*, Tokyo, Japan **1999**, pp. 107–114.
- [15] S. Tachi, K. Tanie, K. Komoriya, M. Abe, *IEEE Trans. Biomed. Eng.* **1985**, *BME-32*, 461.
- [16] H. Kajimoto, in *SIGGRAPH Asia 2012 Emerging Technologies*, Association for Computing Machinery, Singapore **2012**, pp. 1–3.
- [17] A. Gescheider, S. J. Bolanowski, K. R. Hardick, *Somatosensory & Motor Research* **2001**, *18*, 191.
- [18] C. Hatzfeld, R. Werthschützky, in *Haptics: Perception, Devices, Mobility, and Communication* (Eds: P. Isokoski, J. Springare), Springer, Berlin, Heidelberg **2012**, pp. 193–204.
- [19] H. S. Lee, H. Phung, D.-H. Lee, U. K. Kim, C. T. Nguyen, H. Moon, J. C. Koo, J. Nam, H. R. Choi, *Sens. Actuators, A* **2014**, *205*, 191.
- [20] S. J. Lederman, R. L. Klatzky, *Atten., Percept., Psychophys.* **2009**, *71*, 1439.
- [21] D. Leonardis, M. Solazzi, I. Bortone, A. Frisoli, *IEEE Trans. Haptics* **2017**, *10*, 305.
- [22] A. Girard, M. Marchal, F. Gosselin, A. Chabrier, F. Louveau, A. Lécuyer, *Frontiers in ICT* **2016**, *3*, 3.
- [23] S. B. Schorr, A. M. Okamura, *IEEE Trans. Haptics* **2017**, *10*, 418.
- [24] J. J. Zarate, H. Shea, *IEEE Trans. Haptics* **2017**, *10*, 106.
- [25] X. Yu, Z. Xie, Y. Yu, J. Lee, A. Vazquez-Guardado, H. Luan, J. Ruban, X. Ning, A. Akhtar, D. Li, B. Ji, Y. Liu, R. Sun, J. Cao, Q. Huo, Y. Zhong, C. Lee, S. Kim, P. Gutruf, C. Zhang, Y. Xue, Q. Guo, A. Chempakasseril, P. Tian, W. Lu, J. Jeong, Y. Yu, J. Cornman, C. Tan, B. Kim, K. Lee, X. Feng, Y. Huang, J. A. Rogers, *Nature* **2019**, *575*, 473.
- [26] N. Besse, S. Rosset, J. J. Zarate, H. Shea, *Adv. Mater. Technol.* **2017**, *2*, 1700102.
- [27] J. Kang, J. Lee, H. Kim, K. Cho, S. Wang, J. Ryu, *IEEE Trans. Haptics* **2012**, *5*, 21.
- [28] J. J. Huaroto, E. Suarez, H. I. Krebs, P. D. Marasco, E. A. Vela, *IEEE Robot. Autom. Lett.* **2019**, *4*, 17.
- [29] J. Barreiros, H. Claire, B. Peele, O. Shapira, J. Spjut, D. Luebke, M. Jung, R. Shepherd, *IEEE Robot. Autom. Lett.* **2019**, *4*, 277.
- [30] H. A. Sonar, A. P. Gerratt, S. P. Lacour, J. Paik, *Soft Robot.* **2020**, *7*, 22.
- [31] H. Boys, G. Frediani, M. Ghilardi, S. Poslad, J. C. Busfield, F. Carpi, in *IEEE Int. Conf. Soft Robotics (RoboSoft)*, IEEE, Livorno, Italy, **2018**, pp. 270–275.
- [32] G. Frediani, D. Mazzei, D. E. De Rossi, F. Carpi, *Front. Bioeng. Biotechnol.* **2014**, *2*, 31.
- [33] S. Mun, S. Yun, S. Nam, S. K. Park, S. Park, B. J. Park, J. M. Lim, K.-U. Kyung, *IEEE Trans. Haptics* **2018**, *11*, 15.
- [34] K. Jun, J. Kim, I.-K. Oh, *Small* **2018**, *14*, 1801603.
- [35] S. Yun, X. Niu, Z. Yu, W. Hu, P. Brochu, Q. Pei, *Adv. Mater.* **2012**, *24*, 1321.
- [36] I. Koo, K. Jung, J. Koo, J. Nam, Y. Lee, H. R. Choi, *Proc. 2006 IEEE Int. Conf. Robotics and Automation*, ICRA 2006, Orlando, FL **2006**, pp. 2220–2225.
- [37] E. Leroy, R. Hinchet, H. Shea, *Adv. Mater.* **2020**, *32*, 2002564.
- [38] L. Hines, K. Petersen, G. Z. Lum, M. Sitti, *Adv. Mater.* **2017**, *29*, 1603483.
- [39] J. Lin, R. Hinchet, H. Shea, C. Majidi, *Adv. Funct. Mater.* **2020**.
- [40] <https://haptx.com> (accessed: September 2020).
- [41] R. Pelrine, *Science* **2000**, *287*, 836.
- [42] L. Maffii, S. Rosset, M. Ghilardi, F. Carpi, H. Shea, *Adv. Funct. Mater.* **2015**, *25*, 1656.
- [43] J. Huang, T. Li, C. Chiang Foo, J. Zhu, D. R. Clarke, Z. Suo, *Appl. Phys. Lett.* **2012**, *100*, 041911.
- [44] S. Rosset, H. R. Shea, *Appl. Phys. Rev.* **2016**, *3*, 031105.
- [45] H. Zhao, A. M. Hussain, A. Israr, D. M. Vogt, M. Duduta, D. R. Clarke, R. J. Wood, *Soft Robot.* **2020**, *7*, 451.
- [46] X. Ji, X. Liu, V. Cacucciolo, M. Imboden, Y. Civet, A. E. Haitami, S. Cantin, Y. Perriard, H. Shea, *Sci. Robot.* **2019**, *4*, eaaz6451.
- [47] X. Ji, A. E. Haitami, F. Sorba, S. Rosset, G. T. M. Nguyen, C. Plesse, F. Vidal, H. R. Shea, S. Cantin, *Sens. Actuators, B* **2018**, *261*, 135.
- [48] S. Rosset, O. a. Araromi, S. Schlatter, H. R. Shea, *J. Vis. Exp.* **2016**, *108*, e53423.
- [49] M. Imboden, E. de Coulon, A. Poulin, C. Dellenbach, S. Rosset, H. Shea, S. Rohr, *Nat. Commun.* **2019**, *10*, 834.
- [50] A. Poulin, S. Rosset, H. R. Shea, *Appl. Phys. Lett.* **2015**, *107*, 244104.
- [51] D. McCoull, W. Hu, M. Gao, V. Mehta, Q. Pei, *Adv. Electron. Mater.* **2016**, *2*, 1500407.
- [52] S. Rosset, H. R. Shea, *Appl. Phys. A: Mater. Sci. Process.* **2013**, *110*, 281.
- [53] F. Beco, H. Shea, *Smart Mater. Struct.* **2020**, *29*, 10.
- [54] R. S. Johansson, J. R. Flanagan, *Nat. Rev. Neurosci.* **2009**, *10*, 345.
- [55] S. Pourazadi, A. Shagerdmootaab, H. Chan, M. Moallem, C. Menon, *Smart Mater. Struct.* **2017**, *305*, 54.